Computational treatments of cavitation effects in near-free-surface underwater shock analysis

Michael A. Sprague and Thomas L. Geers
Center for Acoustics, Mechanics and Materials, Department of Mechanical Engineering, University of Colorado at Boulder, Boulder, CO 80309-0427, USA
Tel.: +1 303 492 0229; Fax: +1 303 492 3498;
E-mail: Michael.Sprague@Colorado.edu

Fluid cavitation constitutes an expensive computational nuisance in underwater-shock response calculations for structures at or just below the free surface. In order to avoid the use of a large array of cavitating acoustic finite elements (CAFE), various wet-surface approximations have been proposed. This paper examines the performance of two such approximations by comparing results produced by them for 1-D canonical problems with corresponding results produced by more rigorous CAFE computations. It is found that the fundamental limitation of wet-surface approximations is their inability to capture fluid-accretion effects. As an alternative, truncated CAFE fluid meshes with plane-wave radiation boundaries are shown to give good results. In fact, a single layer of CAFE is found to be comparable in accuracy to the better of the wet-surface approximations. The paper concludes with an examination of variations in CAFE modeling.

Keywords: Cavitation, underwater shock, fluid-structure interaction

1. Introduction

When an underwater explosion occurs near a free surface, reflection of the pressure wave causes a large region of bulk cavitation. This cavitated region has substantial influence on the response of marine structures located near or on the free surface, and must therefore be considered [10,11]. One technique for treating the effects of cavitated fluid on structural response is to incorporate a wet-surface approximation (WSA) that applies zero fluid pressure to the wet surface when the fluid is cavitated and uses an acoustics-based approximation otherwise. Previous evaluations of such approximations have been carried out, but have been limited to single-degree-of-freedom (DOF) structural models [2,6–8]. A more rigorous alternative to the use of a WSA is to model the fluid with cavitating acoustic finite elements (CAFE) [3], with the domain outside the CAFE mesh represented by boundary elements based on a doubly asymptotic approximation (DAA) [4,5]. Some 2-D near-free-surface structural-response calculations have demonstrated that the CAFE mesh may be truncated severely in the horizontal direction [11].

In this paper, we evaluate the performance of two WSAs and truncated CAFE meshes with a 1-D, 2-DOF model of a hull supporting internal structure. The model is excited by a plane step-exponential wave propagating vertically. Benchmark response solutions are generated with refined CAFE meshes that suitably contain the cavitation region. Calculations are performed with a research CAFE code based on the displacement-potential formulation of [3].

2. Problem description

The simplest system for studying fluid-structure interaction (FSI) with fluid cavitation incorporates a 1-D fluid column in a rigid pipe with constant cross-sectional area A. We use a 2-DOF spring-mass oscillator floating on the fluid column shown as a CAFE representation in Fig. 1. The column is closed at the bottom by a plane-wave (PW) boundary, which is exact for 1-D acoustic waves. The lower and upper masses, M_1 and M_2, experience velocities V_1 and V_2, respectively; the masses are connected by a linear spring with stiffness K. D is the depth of the CAFE mesh from the wet surface of M_1, x denotes a depth relative to that wet surface, Δx is the length of a 1-D CAFE element, ρ is the fluid density, c is the acoustic velocity, g is the acceleration of gravity, and P_{ATM} is the atmospheric

Shock and Vibration 7 (2001) 105–122
ISSN 1070-9622 / $8.00

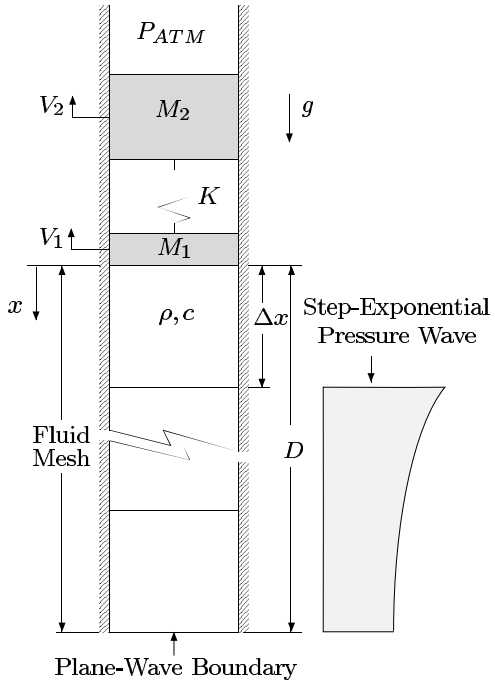

Fig. 1. CAFE-model schematic for a 2-mass oscillator floating on a fluid column.

pressure. The structure is excited by a plane, upward-propagating, step-exponential wave with peak pressure P_{MAX} and decay time τ. At t = 0, the wave front is located one fluid element below the wet surface of M_1.

3. CAFE-model validation

The problem represented in Fig. 1 was solved for $M_2 = 0$ by Bleich and Sandler [1], who applied the method of characteristics to a continuum model of the fluid. Their results are used here to validate our CAFE implementation for the following physical and mesh parameters: $\rho = 989$ kg m^{-3} (9.3455$\times 10^{-5}$ lb sec^2 in^{-4}), $c = 1451$ m/sec (57,120 in/sec), $P_{ATM} = 0.101$ MPa (14.7 psi), $g = 9.81$ m sec^{-2} (386.4 in sec^{-2}), $P_{MAX} = 0.710$ MPa (103 psi), $\tau = 0.9958$ msec, $D = 3.81$ m (150 in), and $d = 0.145$ m (5.70 in) where d is the equilibrium draft of a corresponding 3-D floating structure. The CAFE artificial-fluid-damping factor β (see [3]) was taken as 0.5. Explicit time integration was performed with a fixed time increment Δt equal to half the Courant-Friedrichs-Levy increment limit ($\Delta t_{CFL} = \Delta x/c$). The actual time-increment limit Δt_{crit} is slightly smaller than Δt_{CFL} due to the artificial damping and coupling between the structure and PW boundary [3]. It has been found that $\Delta t = \Delta t_{CFL}/2$ yields excellent results, and, unless otherwise noted, is used in all of the calculations. The above parameters are equivalent to those used by Felippa and DeRuntz [3] to validate the CAFE formulation.

Figure 2(a) shows M_1 velocity-response histories found in [1] and those calculated with CAFE models ($\Delta x = 38.1$ mm and $\Delta x = 10$ mm). The $\Delta x = 38.1$ mm element size was chosen to agree with that used in [3] to validate the CAFE method. Response histories were calculated with and without the inclusion of cavitation effects to demonstrate the large influence that cavitation has on structure response. The space-time cavitation zone found in [1] and those calculated with $\Delta x = 38.1$ mm and $\Delta x = 10$ mm are shown in Figs 2(b) and (c), respectively, where horizontal lines defining the CAFE cavitation zone consist of dots that record when absolute pressure at a node is zero.

It should be noted that effects below the upper boundary of the cavitation region do not affect the velocity response of M_1, as disturbances cannot propagate through a cavitated region of fluid. We define *fluid accretion* as the presence of an uncavitated region of fluid residing between the structure and a region of cavitated fluid. Figures 2(b) and (c) show fluid accretion

occurring in the Bleich and Sandler solution [1] between 0.3 and 10.1 msec. *Cavitation closure* has long been defined as the event in which the upper and lower cavitation-region boundaries converge. The time-space location of this event is denoted by (t_c, x_c) and occurs in the Bleich and Sandler solution at (10.1 msec, 2.14 m). The cavitation-zone plots also contain several characteristic curves defined by $|dx/dt| = c$. Disturbances in the fluid propagate along characteristic curves that parallel those shown. Finally, we define γ_c as the ratio of the accreted fluid mass at the time of initial closure to M_1, i.e.,

$$\gamma_c = \frac{\rho x_c A}{M_1}. \tag{1}$$

With cavitation effects neglected, the CAFE-response histories are indistinguishable from the closed-form solution. With cavitation effects included, the CAFE results are seen to agree well with the Bleich and Sandler solution. However, the $\Delta x = 38.1$ mm solution fails to reproduce accurately the sharp change in velocity at $t \approx 11$ msec. From the characteristic lines in Figs 2(b) and (c), it is clear that this change in velocity is associated with the pressure pulse generated by closure. The $\Delta x = 10$ mm solution obviously reproduces the Bleich and Sandler cavitation zone and M_1 velocity response with better accuracy than does the $\Delta x = 38.1$ mm solution. Finally, we note the existence of a small region of cavitation protruding from the lower cavitation boundary in Fig. 2(b) at $t \approx 3$ msec. This region is much smaller in the refined-mesh calculation of Fig. 2(c). The characteristic line from (2.7 msec, 3.8 m) to (3.2 msec, 3.0 m) shows that this artifact results from the impedance mismatch between the mildly dispersive CAFE mesh and the exact PW boundary.

4. 1-D wet-surface approximations

The total force acting upward on M_1 in the absence of cavitation is

$$F_1 = -M_1 g - AP_{ATM} - F_K + AP_{FF} + AP_S, \tag{2}$$

where P_S is the scattered fluid pressure, F_K is the force exerted by the spring, and P_{FF} is the absolute free-field pressure. The free field is that which exists when the structure is removed and replaced with fluid. When there are no regions of cavitation in the 1-D fluid column, FSI effects may be treated rigorously with the PW radiation boundary, for which the relationship between P_S and scattered fluid velocity U_S is given by

$$P_S = \rho c U_S. \tag{3}$$

If regions of cavitation exist below M_1, the force Eq. (2) becomes an approximation that may involve substantial error. However, if the region of fluid in contact with the floating mass drops to its vapor pressure P_{VAP}, the fluid cavitates and the total force acting on M_1 becomes

$$F_1 = -M_1 g - AP_{ATM} - F_K + AP_{VAP}. \tag{4}$$

The "free-fall" condition Eq. (4) is the basis for the two WSAs evaluated in this paper. These approximations use a total force on M_1 defined by Eq. (2) when the fluid at the wet surface is not cavitated and Eq. (4) otherwise; as P_{VAP} is small, it is usually neglected. The differences between the WSAs considered here lie in the determination of the cavitation-onset time $t_{\rm on}$ and cavitation-closure time $t_{\rm off}$.

The first approximation, denoted by PZ-on/PZ-off, uses zero crossings of calculated absolute fluid pressure $P_{FF} + P_S$ to determine $t_{\rm on}$ and $t_{\rm off}$. The second approximation, presented by DiMaggio et al. [2] and Sandler [8] and denoted by PZ-on/SC-off, uses the following separation-closure criterion to determine t_{off}:

$$\int_{t_{\rm on}}^{t_{\rm off}} (V_1 - U_{FF}) dt = 0, \tag{5}$$

where U_{FF} is the free-field fluid velocity at d.

The free-field data used in the WSAs were determined with a highly refined CAFE model of the fluid. A $D = 6$ m (236 in) fluid column with $\Delta x = 0.2$ mm (0.008 in), $\rho = 1025$ kg m^{-3} (0.9593×10^{-4} lb sec^2 in^{-4}), $c = 1500$ m sec^{-1} (59055 in sec^{-1}), $P_{ATM} = 0.101$ MPa (14.7 psi), and $g = 9.81$ m sec^{-2} (386.4 in sec^{-2}) was used. A draft $d = 5.08$ m (200 in) was chosen as the baseline case for the floating structure. The parameters for the incident wave were chosen to correspond to a 45.4 kg (100 lb) charge of HBX-1 at a depth of 15.2 m (50 ft) which, in conjunction with the 5.08 m draft, produces a standoff of 10.1 m (33.3 ft). This produces a spherical step-exponential wave with $P_{MAX} = 16.15$ MPa (2343 psi) and $\tau = 0.423$ msec [9]. These values were applied to the plane step-exponential wave used for excitation in all subsequent calculations. The resulting free field at the 5.08 m depth is shown in Fig. 3. We see that, after the incident wave decays essentially to zero at $t \approx 3$ msec, the free-field pressure returns to the ambient pressure ($P_{ATM} + \rho g d$) until a wave is reflected from the surface at $t = 7$ msec. Although a region of fluid above d cavitates, the fluid at d experiences only positive pressure and does not cavitate. The peaks in

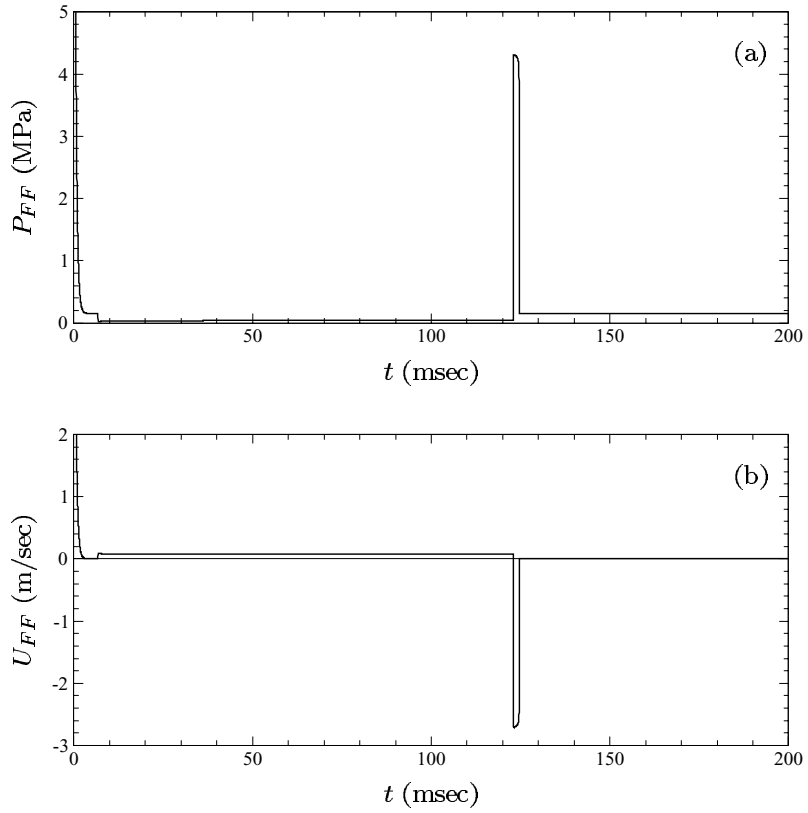

Fig. 3. Free-field results used in the WSA calculations. Free-field (a) absolute pressure and (b) velocity at the CAFE node 5.08 m below the surface.

P_{FF} and U_{FF} at $t = 123$ msec are due to the closure of the cavitation region occurring above d.

For the parameters listed above, the responses V_1 and V_2 were calculated "exactly" by the CAFE method with the fluid column extending below the deepest occurrence of cavitation. Several Δx-values were used to ensure a converged solution at $\Delta x = 2.5$ mm. The two WSAs were also employed to calculate V_1 and V_2.

Figure 4(a) shows V_1-response histories for $M_2/M_1 = 0$, a structural model similar to that of DiMaggio et al. [2] and of Sandler [8]. For this and subsequent models, $D = 3$ m was sufficient to capture the entire cavitation region. The figure displays excellent performance by both approximations until $t \approx 70$ msec, but PZ-off nullifies cavitation far too early to be of any value afterward. However, SC-off demonstrates good performance overall. Figure 4b shows the cavitation zone calculated with the CAFE model and explains why the PZ-on/SC-off WSA performs so well. The fluid element directly beneath M_1 remains continuously cavitated for about 45 msec, leaving M_1 in an extended state of free fall, a condition required for satisfactory performance of this WSA. However, at $t \approx 45$ msec the fluid element directly beneath M_1 stops cavitating; this marks the beginning of fluid accretion. Close inspection of the velocity-response histories reveals that this is the time when the CAFE and approximate histories begin to diverge. This is expected, as these WSAs do not account for fluid accretion. However, the mass of the accreted fluid is small relative to M_1 ($x_c = 0.55$ m, $\gamma_c = 0.01$).

A slightly more realistic ship model consists of a hull, M_1, with supported internal structure, $M_2 > 0$. Figures 5(a) and (b) show approximate and CAFE velocity-response histories for $M_2/M_1 = 1$, where the spring stiffness was selected to give M_2 a fixed-base natural frequency of 5 Hz, i.e., $K = (5 \times 2\pi)^2 M_2$. Both wet-surface approximations do well at early time but PZ-off again nullifies cavitation far too early. The PZ-on/SC-off WSA is somewhat in error during $40 < t < 80$ msec, but is otherwise acceptable. V_2 response calculated with PZ-on/SC-off is quite good.

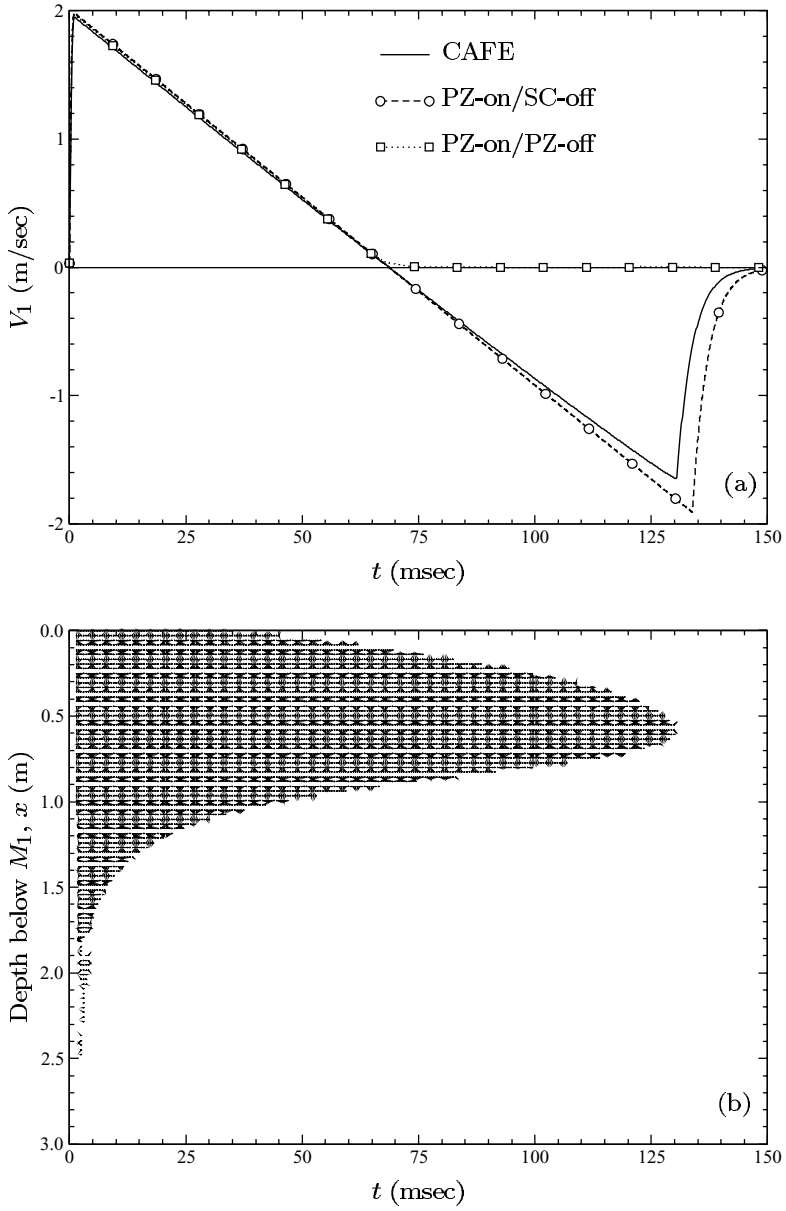

Fig. 4. (a) V_1-response histories for $M_2/M_1 = 0$, demonstrating the performance of two WSAs (PZ – Pressure Zero, SC – Separation Closure). (b) Cavitation zone.

The cavitation-zone plot shown in Fig. 5(c) reveals two distinct cavitation zones and a degree of fluid accretion greater than that observed in the previous calculation ($x_c = 1.0$ m, $\gamma_c = 0.04$). Thus, the performance of the PZ-on/SC-off calculation is slightly poorer.

Figures 6(a) and (b) show V_1- and V_2-response histories, respectively, for $M_2/M_1 = 5$. Other than at early time, both WSAs produce V_1- and V_2-response histories with unacceptable error levels. Figure 6(c) shows two distinct cavitation zones and a large degree of fluid accretion ($x_c = 1.4$ m, $\gamma_c = 0.14$).

Finally, Figs 7(a) and (b) show V_1- and V_2-response histories for $M_2/M_1 = 25$. These histories also demonstrate the complete failure of both WSAs. Figure 7(c) shows the associated cavitation zones, the first of which exhibits a high degree of accretion

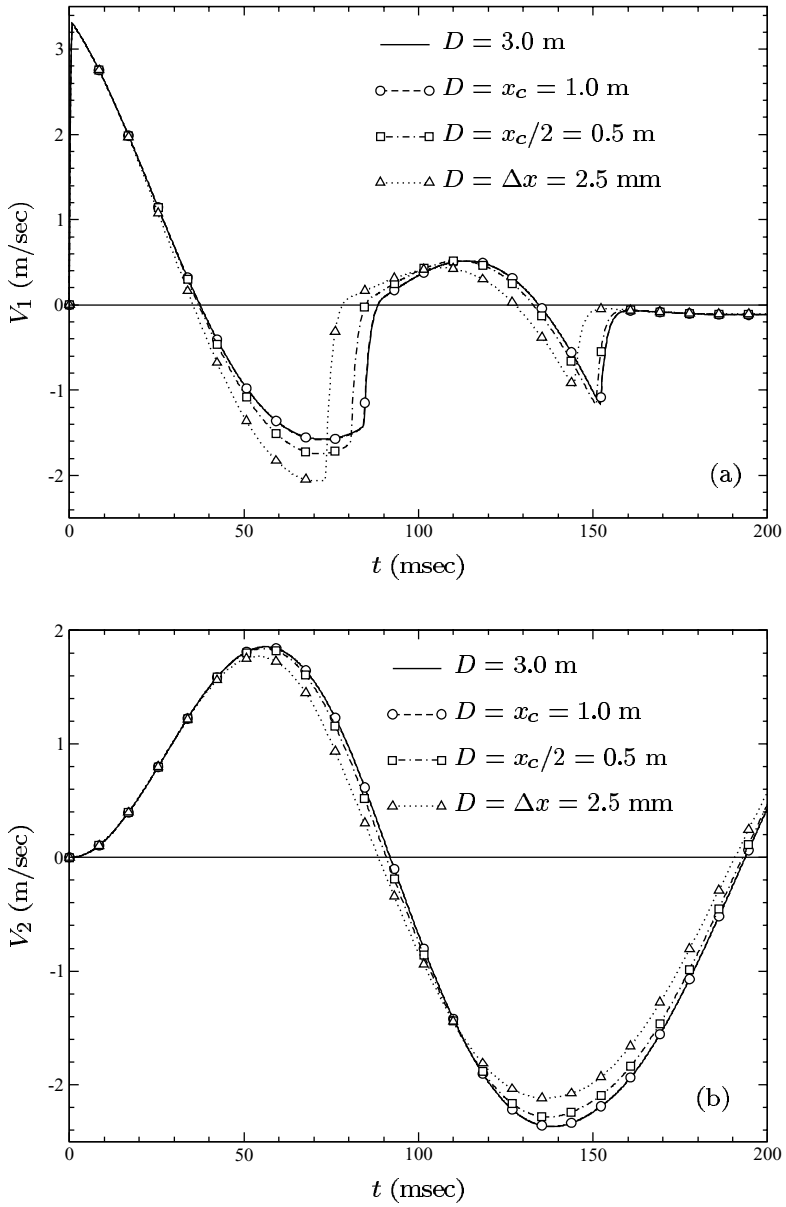

Fig. 8. (a) V_1- and (b) V_2-response histories for $M_2/M_1 = 1$, demonstrating the performance of truncated CAFE meshes.

($x_c = 1.6$ m, $\gamma_c = 0.74$).

5. Truncated CAFE meshes

The previous section reveals that the PZ-on/PZ-off WSA is generally unsatisfactory and that the PZ-on/SC-off WSA fails as the wet portion of the structure becomes increasingly buoyant. Therefore, CAFE discretization of the fluid column emerges as the most reliable existing method for treating cavitation. However, discretization of the entire domain in which cavitation occurs may be prohibitively expensive. Hence, it is important to determine whether such discretization is actually necessary.

Figures 8(a) and (b) show V_1- and V_2-response histories for $M_2/M_1 = 1$, calculated with various CAFE-discretization depths. It is seen that a model with a

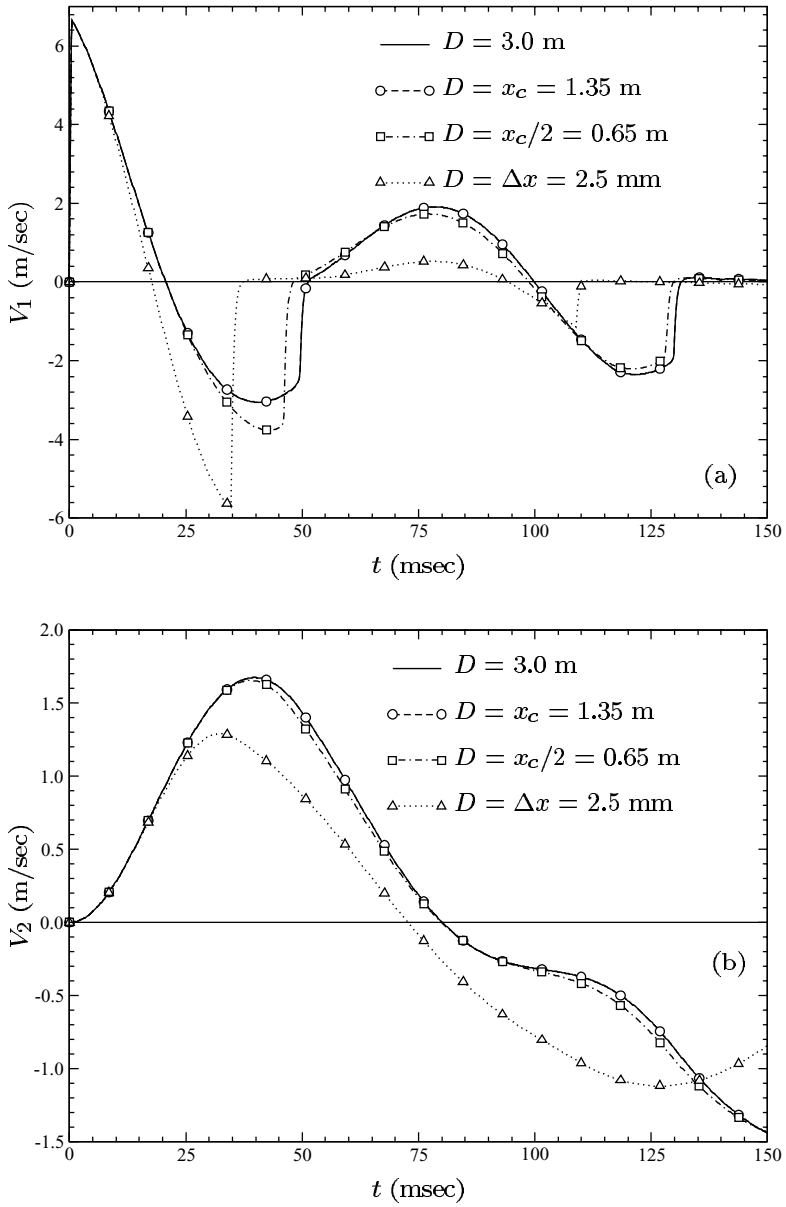

Fig. 9. (a) V_1- and (b) V_2-response histories for $M_2/M_1 = 5$, demonstrating the performance of truncated CAFE meshes.

truncation boundary that lies at the point of maximum accretion ($D = x_c$) produces a velocity response that is identical to that calculated with a truncation boundary that encloses the entire cavitation region. In fact, the CAFE model that captures only half the accretion region ($D = x_c/2$) produces good results. Even a single CAFE element ($D = \Delta x$) produces adequate results. Similar performance is demonstrated by the $D = x_c$ and $D = x_c/2$ calculations in Fig. 9 for $M_2/M_1 = 5$ and in Fig. 10 for $M_2/M_1 = 25$. However, the $D = \Delta x$ velocity responses in Figs 9 and 10 exhibit substantial error.

Now we directly compare results produced by the PZ-on/SC-off approximation with those produced by truncated CAFE meshes. Figure 11 shows velocity-response histories selected from the (a)-portions of Figs 5–10. It is clear that the PZ-on/SC-off approximation is no match for the CAFE mesh truncated at

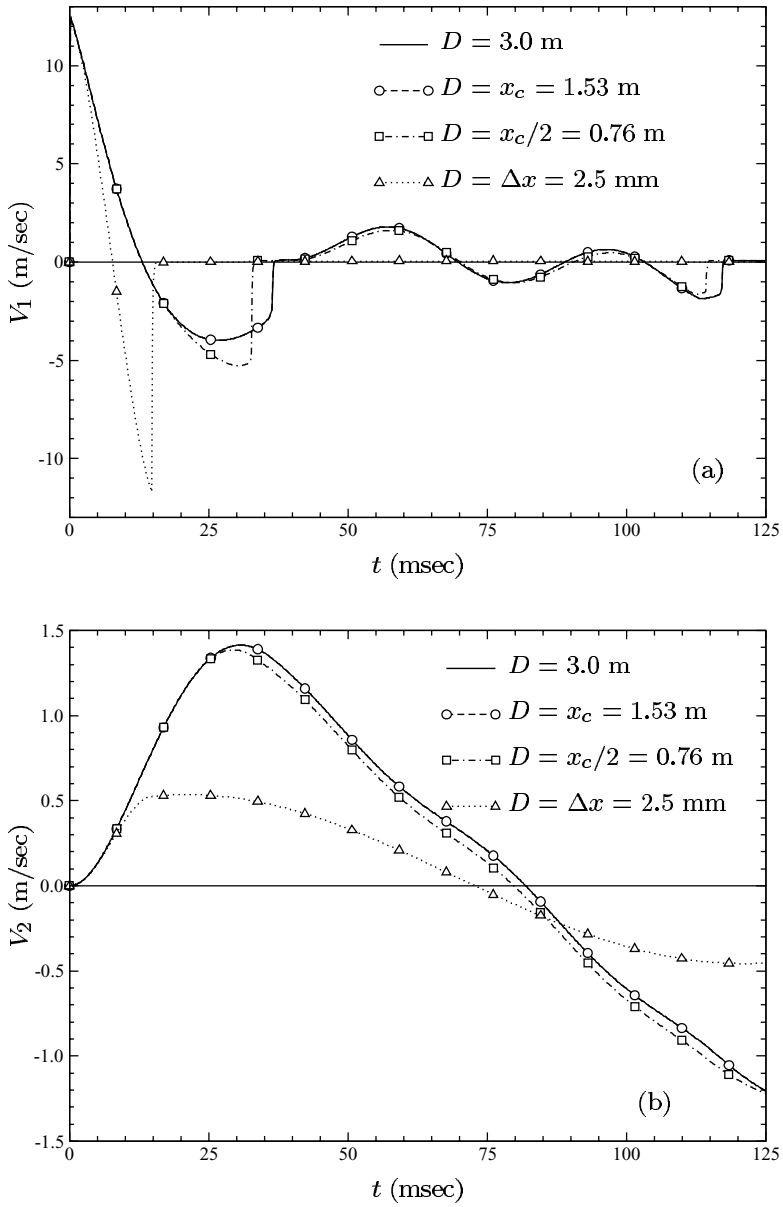

Fig. 10. (a) V_1- and (b) V_2-response histories for $M_2/M_1 = 25$, demonstrating the performance of truncated CAFE meshes.

$D = x_c/2$. In fact, it is very nearly equivalent to the use of a single layer of cavitating acoustic finite elements ($D = \Delta x$).

6. CAFE modeling

Having demonstrated the need for CAFE discretization of a portion of the fluid domain, we proceed to investigate several CAFE-implementation issues employing the 1-D system with $M_2/M_1 = 5$. Unless otherwise noted, the CAFE models use $D = 3$ m, $\Delta x = 2.5$ mm, $\Delta t = \Delta t_{CFL}/2$, and $\beta = 0.5$.

6.1. Time increment

Because the fixed-base natural frequency was low in the models considered above, the critical time incre-

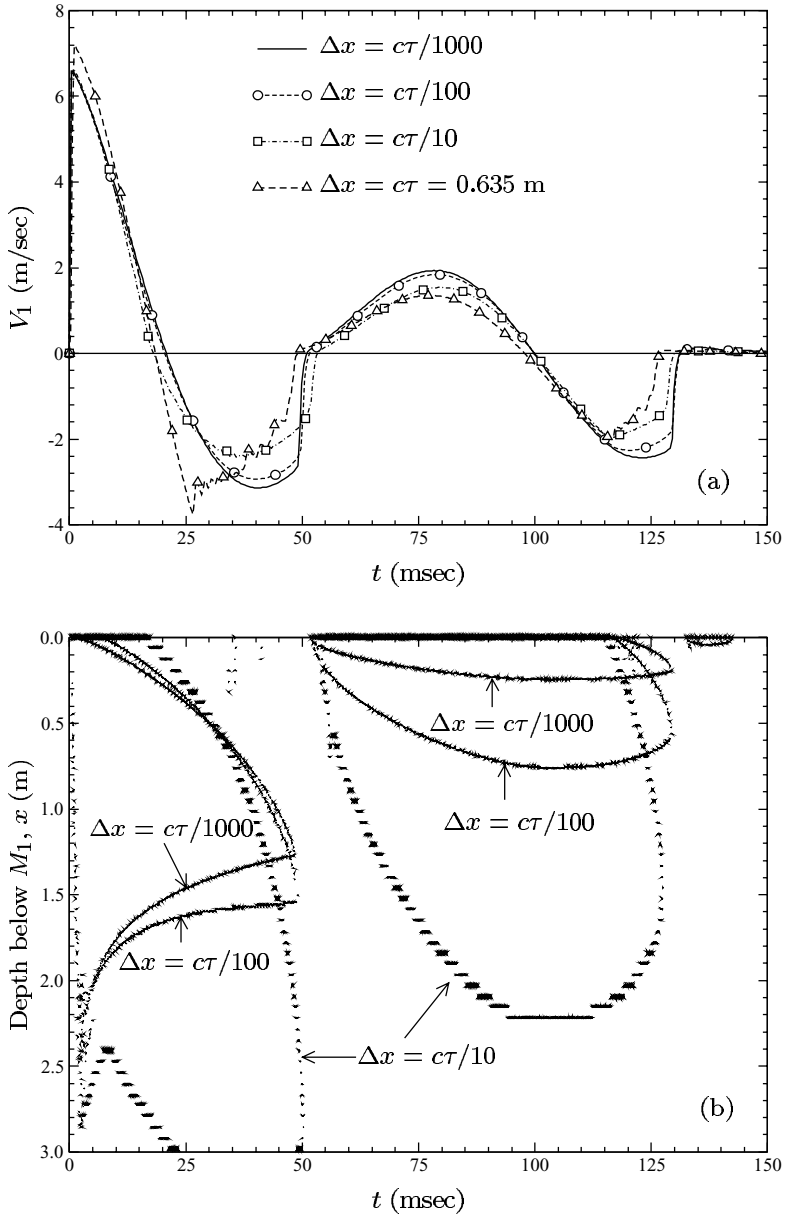

Fig. 13. (a) V_1-response histories for $M_2/M_1 = 5$ calculated with various Δx values. (b) Fluid-change-of-phase plot.

ment Δt_{crit} for stable integration was governed by the CAFE elements. However, in many coupled CAFE/FE models with explicit-fluid/explicit-structure time integration, Δt_{crit} is likely to be governed by the structural elements. This may be detrimental, as time integration of the CAFE equations is most accurate when Δt is close to Δt_{crit} for the CAFE mesh. Figure 12(a) shows V_1-response histories calculated with two Δt-values. Figure 12(b) shows a fluid-change-of-phase plot for the $\Delta t = 0.5\Delta t_{CFL}$ calculation. A dot in this figure indicates a change of phase from one node to another or from one time step to the next. This produces outlines of the cavitation zones shown in Fig. 6(c). Figure 12(c) shows a similar change-of-phase plot for the $\Delta t = 0.05\Delta t_{CFL}$ calculation. We observe much fluctuation of fluid between the cavitated and uncavitated

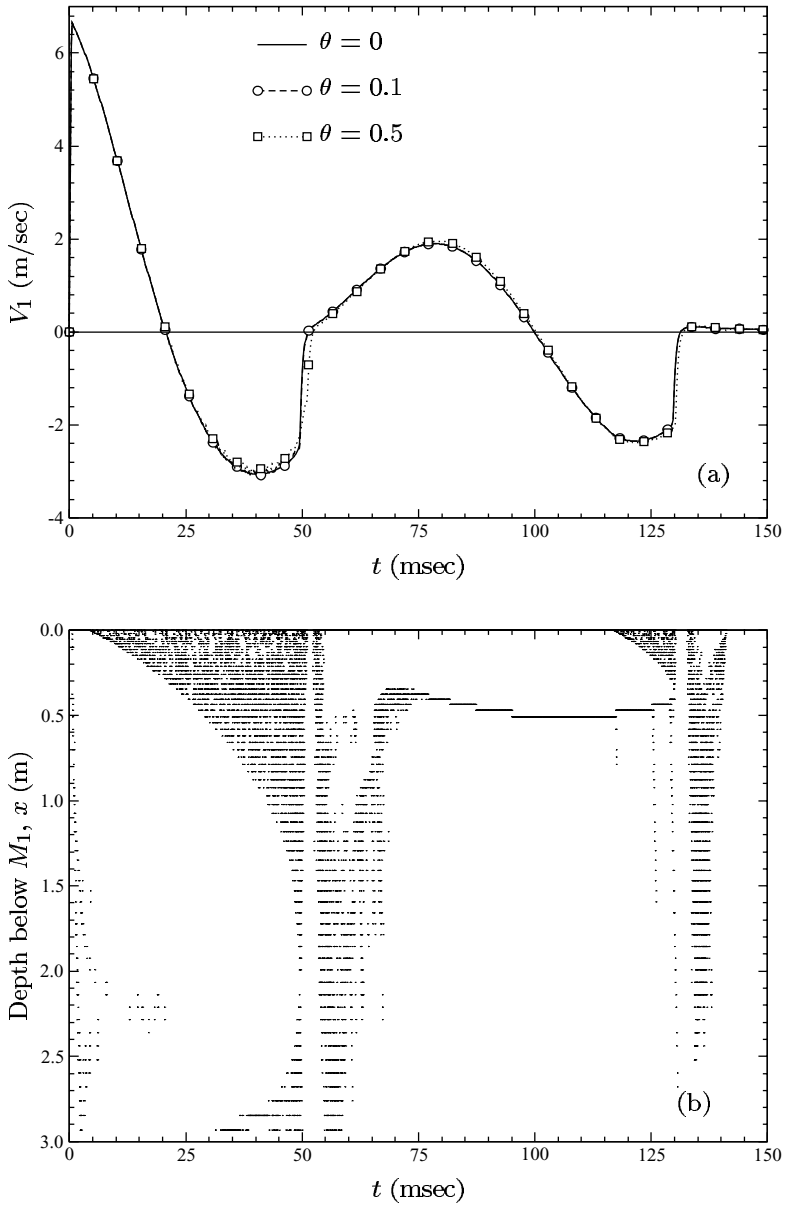

Fig. 14. (a) V_1-response histories for $M_2/M_1 = 5$ calculated with three θ values. (b) Fluid-change-of-phase plot for $\theta = 0.5$.

state, a numerical artifact that has been termed *frothing* [3]. Although the frothing in Fig. 12(c) is quite severe, however, its effect on the response of M_1 is small. Nevertheless, it would be desirable in engineering calculations to be able to integrate the structural equations of motion with a time increment substantially smaller than that employed to integrate the fluid equations of motion.

6.2. Element size

Figure 13(a) shows V_1-response histories for $M_2/M_1 = 5$ calculated with various element dimensions, expressed as the number of elements per incident-wave decay length ($c\tau$). Figure 13(b) shows the fluid-change-of-phase plots for several mesh-refinement levels. It is interesting to note that, although the cavitation zones

exhibit large differences, the velocity-response histories are quite similar.

6.3. Mesh gradation

When modeling 2-D or 3-D problems with CAFE, it is common to use a mesh gradation that increases the element dimensions with increasing distance from the structure. These variable-sized CAFE elements have Δt_{crit} values that may differ greatly from those near the structure. Here we use the 1-D problem to investigate the performance of a nonuniform CAFE mesh and its effect on structural response. Specifically, we employ a CAFE mesh with element sizes defined by $\Delta x_n = \Delta x + (n-1)\theta\Delta x$, where Δx_n is the length of the n^{th} element from the structure, Δx is the element length adjacent to the structure, and θ determines the degree of mesh gradation. Figure 14(a) shows V_1-response histories calculated with three θ-values and Fig. 14(b) shows the fluid-change-of-phase plot for the $\theta = 0.5$ calculation. Although varying the degree of gradation has little effect on the V_1-response calculations, the use of a nonuniform mesh introduces substantial frothing and yields cavitation plots that are bizarre.

6.4. Summary

From Figs 6(c), 12(b), 12(c), 13(b), and 14(b), it is apparent that cavitation in the CAFE mesh depends strongly on the choices of Δt, Δx, and θ. Optimum performance is achieved with a large stable time increment ($\Delta t \approx \Delta t_{CFL}/2$), a high level of spatial refinement ($\Delta x \ll c\tau$), and uniform meshing ($\theta = 0$). However, Figs 12(a), 13(a), and 14(a) show that structural response is insensitive to these choices, which is most fortunate. A similar CAFE-parameter sensitivity study with the Bleich and Sandler [1] problem produces velocity responses that are more sensitive to errors in the CAFE mesh. However, the mass value used by Bleich and Sandler is not representative of those typically encountered in practice.

7. Conclusion

Extensive underwater-shock calculations with cavitating-acoustic-finite-element (CAFE) models for a 1-D, 2-DOF system floating on a fluid column have shown the PZ-on/SC-off approximation of DiMaggio et al. [2] and Sandler [8] to be the better of two wet-surface cavitation approximations considered. However, the accuracy of the PZ-on/SC-off approximation degrades as the ratio of internal mass to hull mass increases. This degradation is caused by the inability of the approximation to account for fluid accretion at the structure's wet surface, and becomes quite pronounced when the internal-to-hull-mass ratio exceeds unity.

For the 1-D cases studied, it is found that a CAFE mesh that merely contains the region of fluid accretion produces structure-response histories that are identical to those produced by a CAFE mesh that contains the entire cavitation region. Furthermore, it is observed that a mesh that contains only half of the accretion region produces adequate results. Finally, it is found that a single-layer CAFE mesh yields results that are equivalent in performance to those produced by the PZ-on/SC-off approximation.

FSI calculations for the 1-D, 2-DOF system demonstrate that the cavitation behavior of the CAFE mesh is strongly dependent on discretization parameters. However, the associated structural-response histories are weakly dependent on those parameters.

Acknowledgment

This research was sponsored by the Defense Threat Reduction Agency under contract DNA-001-94-C-0004 with Mr. Michael Giltrud acting as technical monitor. The authors express their appreciation to Mr. Giltrud and Mr. Douglas Bruder for DTRA's support of this work.

References

[1] H.H. Bleich and I.S. Sandler, Interaction Between Structures and Bilinear Fluids, *International Journal of Solids and Structures* **6** (1970), 617–639.

[2] F.L. DiMaggio, I.S. Sandler and D. Rubin, Uncoupling Approximations in Fluid-Structure Interaction Problems with Cavitation, *Journal of Applied Mechanics* **48** (1981), 753–756.

[3] C.A. Felippa and J.A. DeRuntz, Finite Element Analysis of Shock-Induced Hull Cavitation, *Computer Methods in Applied Mechanics and Engineering* **44** (1984), 297–337.

[4] T.L. Geers, Doubly Asymptotic Approximations for Transient Motions of Submerged Structures, *Journal of the Acoustical Society of America* **64**(5) (1978), 1500–1508.

[5] T.L. Geers and P. Zhang, Doubly Asymptotic Approximations for Submerged Structures with Internal Fluid Volumes, *Journal of Applied Mechanics* **61** (1994), 893–906.

[6] K. Mäkinen, Cavitation Models for Structures Excited by a Plane Shock Wave, *Journal of Fluids and Structures* **12** (1998), 85–101.

[7] M.L. Rehak, F.L. DiMaggio and I.S. Sandler, Interactive Approximations for a Cavitating Fluid Around a Floating Structure, *Computers and Structures* **21**(6) (1985), 1159–1175.

[8] I.S. Sandler, A Method of Successive Approximations for Structure Interaction Problems, in: *Computational Methods for Infinite Domain Media- Structure Interaction*, (Vol. AMD–46), A.J. Kalinowski, ed., ASME, 1981, pp. 67–81.

[9] Y.S. Shin and T.L. Geers, Response of Marine Structures to Underwater Explosions, (Unpublished), Short-Course Notes, Shock and Vibration Research, Monterey, CA, 1999.

[10] Y.S. Shin and L.D. Santiago, Surface Ship Shock Modeling and Simulation: Two-Dimensional Analysis, *Shock and Vibration* **5** (1998), pp. 129–137.

[11] J.E. van Aanhold, G.J. Meijer and P.P.M. Lemmen, Underwater Shock Response Analysis of a Floating Vessel, *Shock and Vibration* **5** (1998), pp. 53–59.

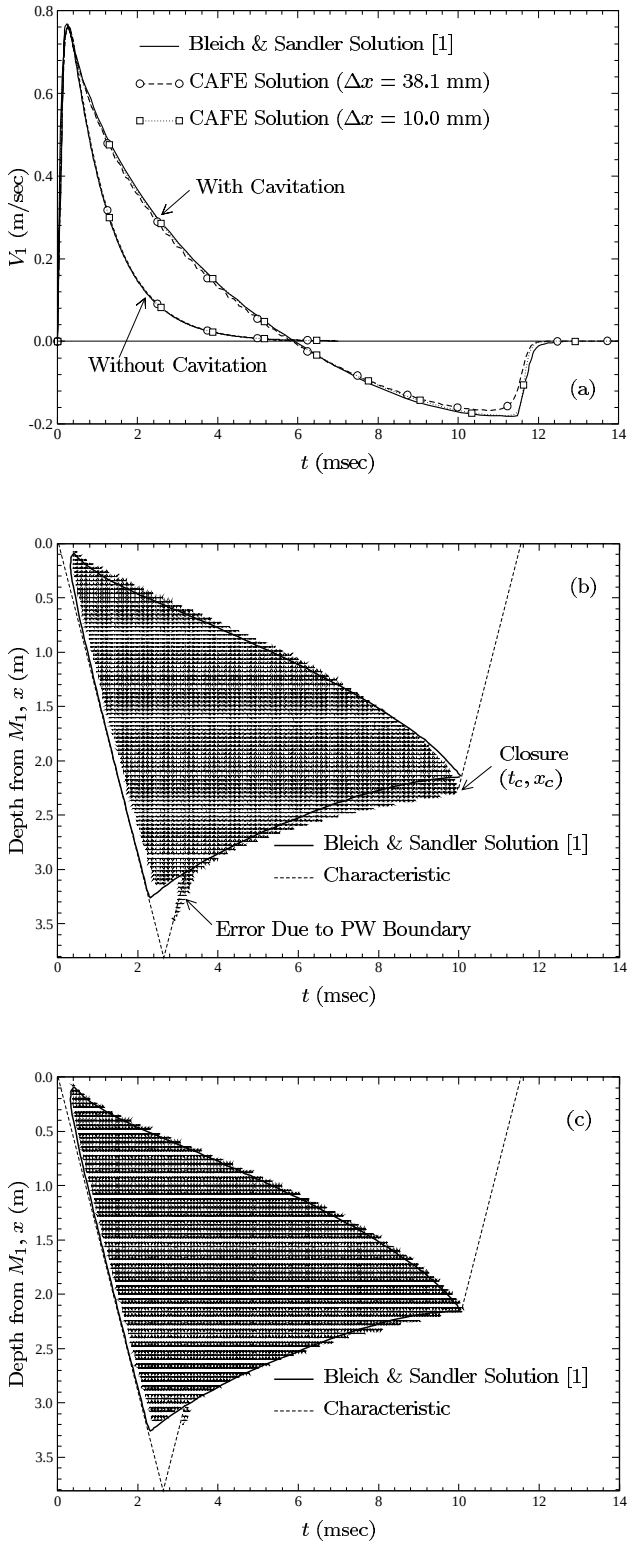

Fig. 2. Validation of the CAFE method with the Bleich and Sandler problem [**?**]. (a) V_1-response histories for $M_2/M_1 = 0$. (b) Cavitation zone; horizontal lines indicate cavitated zone of CAFE model.

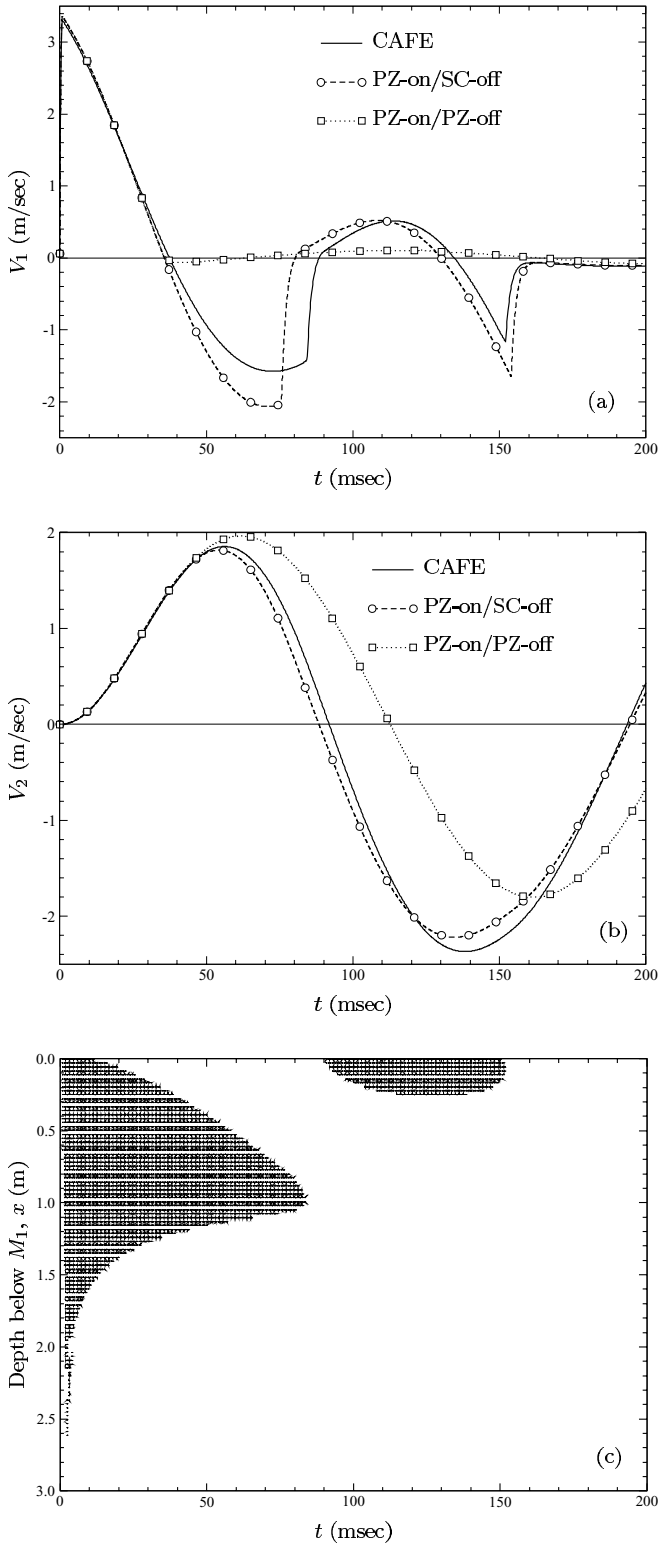

Fig. 5. (a) V_1- and (b) V_2-response histories for $M_2/M_1 = 1$, demonstrating the performance of two WSAs (PZ – Pressure Zero, SC – Separation Closure). (c) Cavitation zone.

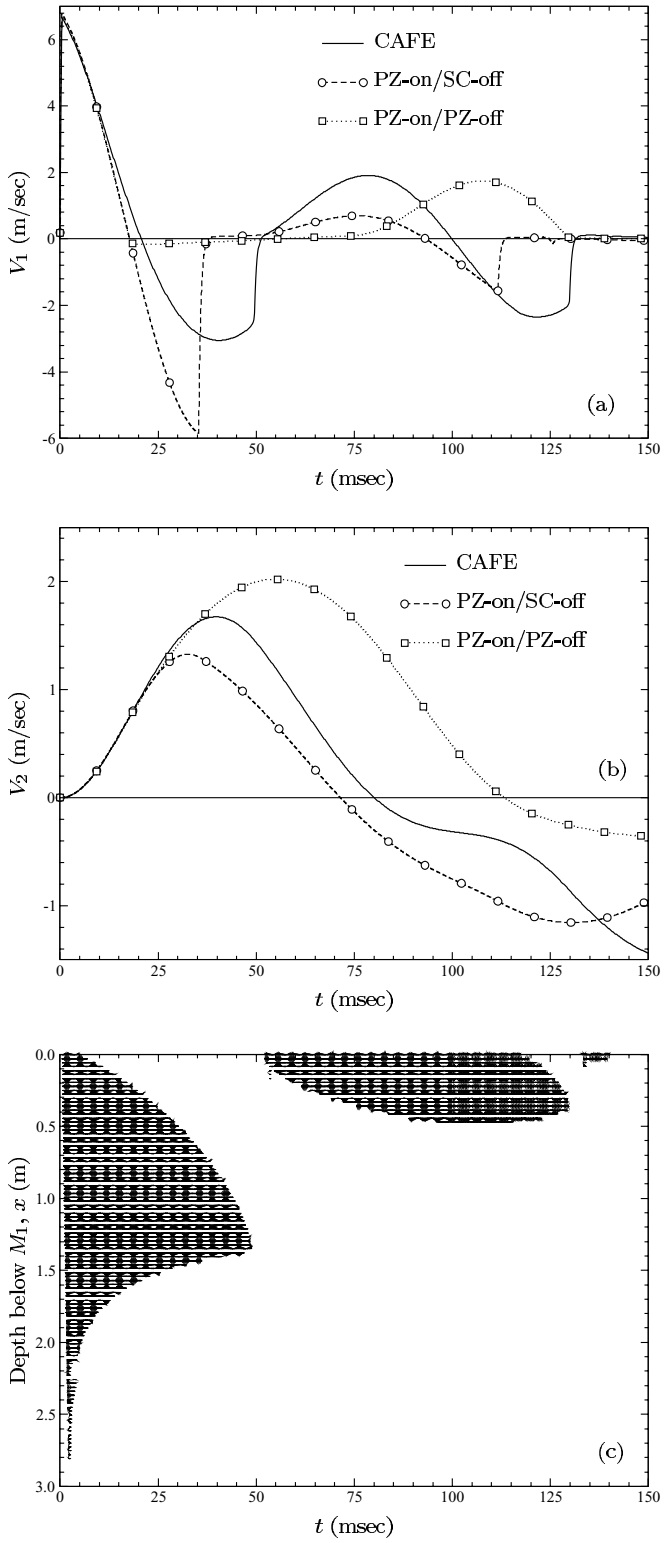

Fig. 6. (a) V_1- and (b) V_2-response histories for $M_2/M_1 = 5$, demonstrating the performance of two WSAs (PZ – Pressure Zero, SC – Separation Closure). (c) Cavitation zone.

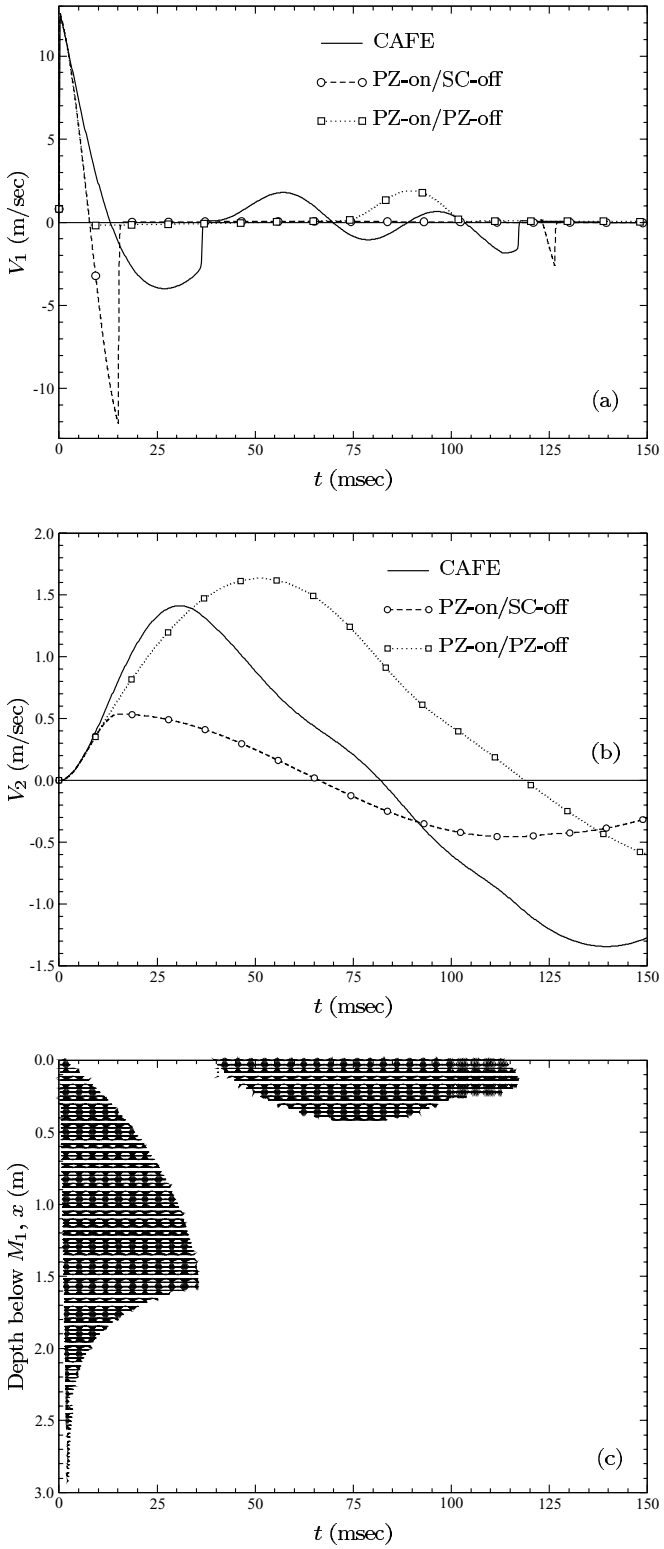

Fig. 7. (a) V_1- and (b) V_2-response histories for $M_2/M_1 = 25$, demonstrating the performance of two WSAs (PZ – Pressure Zero, SC – Separation Closure). (c) Cavitation zone.

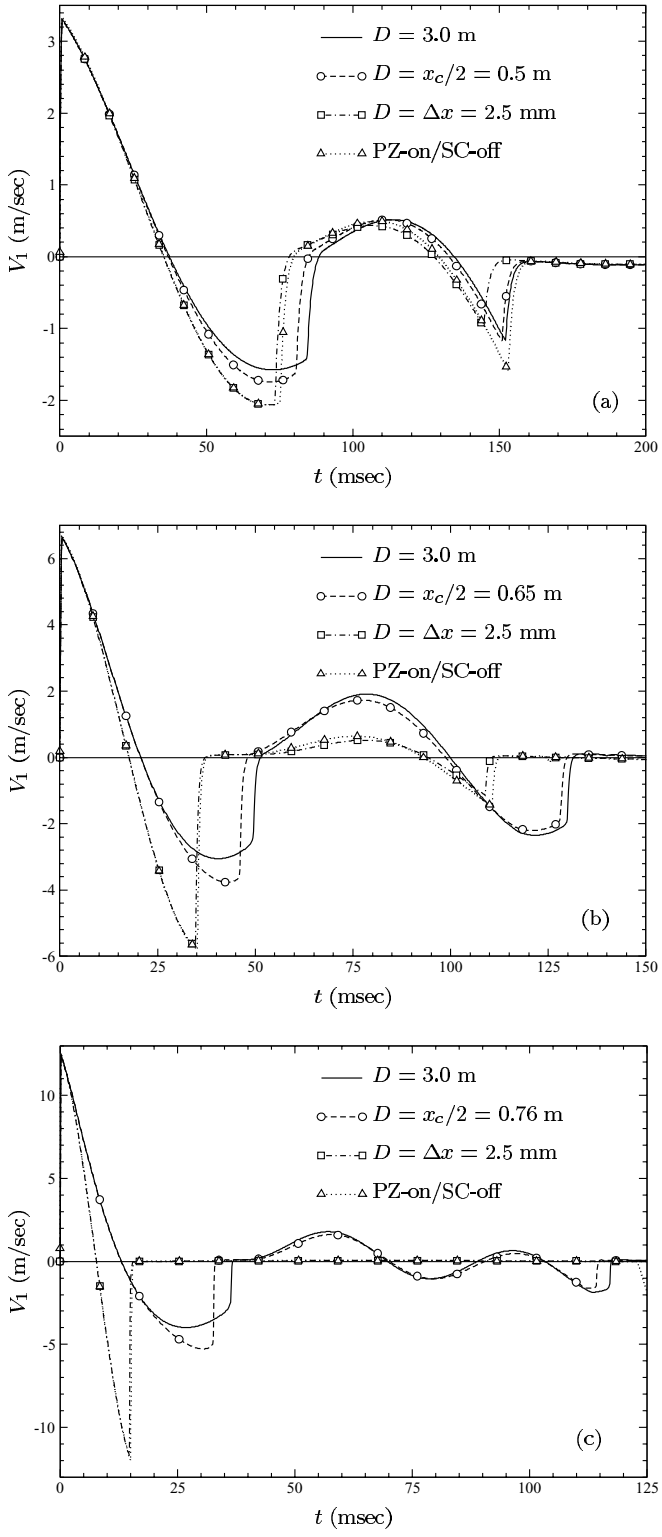

Fig. 11. V_1-response histories for (a) $M_2/M_1 = 1$, (b) $M_2/M_1 = 5$, and (c) $M_2/M_1 = 25$, produced by truncated CAFE meshes and the PZ-on/SC-off WSA.

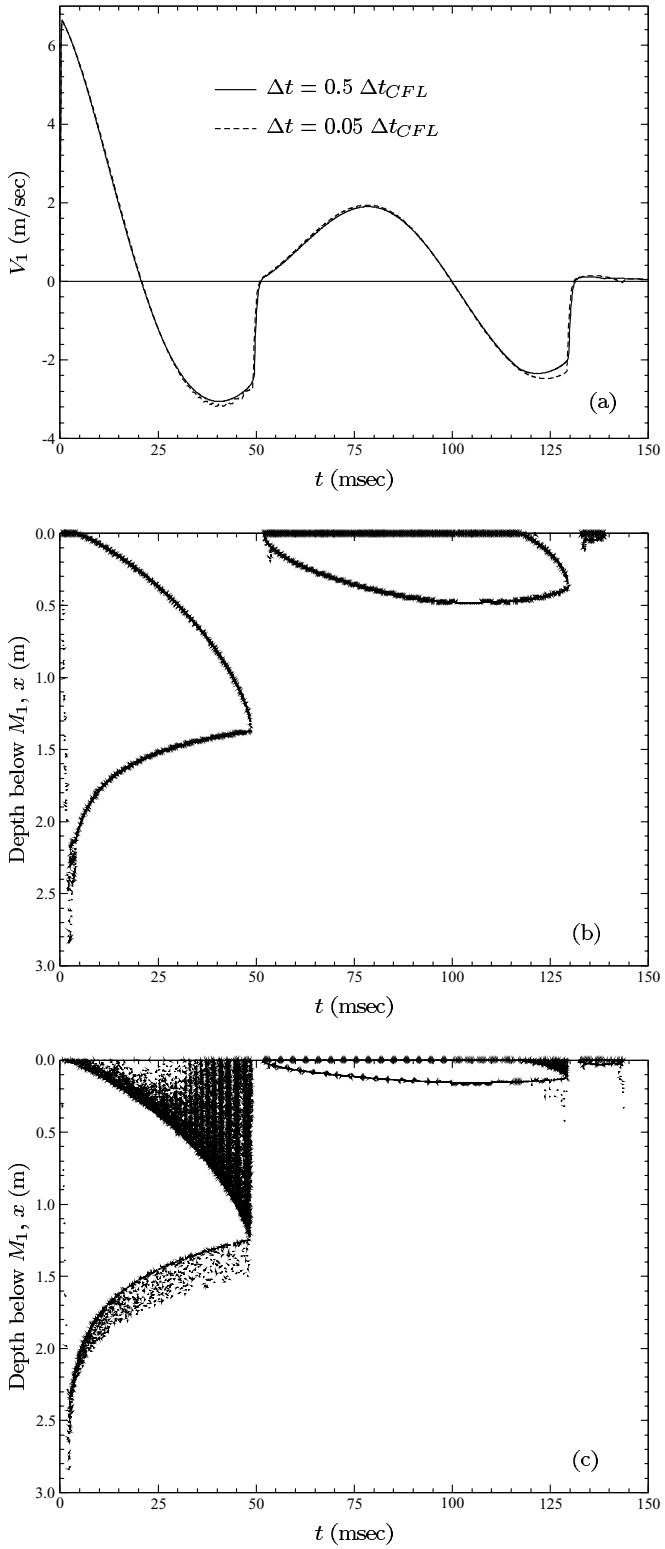

Fig. 12. (a) V_1-response histories for M_2/M_1 = 5 calculated with two Δt values. Fluid-change-of-phase plot for (b) $\Delta t = 0.5\Delta t_{CFL}$ and (c) $\Delta t = 0.05\Delta t_{CFL}$.